

Research progress on mid-IR nonlinear optical crystals with high laser damage threshold in China

Tianxiang ZHU, Xingguo CHEN and Jingui QIN (✉)

Department of Chemistry and Hubei Key Laboratory on Organic and Polymeric Opto-electronic Materials, Wuhan University, Wuhan 430072, China

Nonlinear optical (NLO) crystals have been playing an increasingly important role in laser science and technology. The NLO crystals used in the middle infrared (mid-IR) region, compared with the NLO crystals in the other wavelength regions, are still not good enough for the application of high-energy laser. The main defect is that their laser damage thresholds (LDT) are low. Chinese scientists have made a lot of important contributions to the UV and visible NLO crystals. In the last decade, they also did a lot of work on the mid-IR NLO materials. The main purpose of these researches is to increase the LDT and simultaneously balance the other properties. This paper presents a brief summary of their research progress in this topic on three types of materials: chalcogenides, oxides, and halides. The emphasis is put on the design strategy and quality control of the crystals.

Keywords nonlinear optical (NLO) crystals, laser damage threshold (LDT), mid-IR region, design, crystal growth

1 Introduction

Since the second harmonic generation (SHG) was observed when a ruby laser was directed into a quartz crystal in 1961 [1], nonlinear optical (NLO) crystals have played a key role in the laser frequency conversion, optical parameter oscillation (OPO), and signal communication [2,3]. Some good crystals have been discovered and commercialized for the applications in different wavelength ranges from vacuum UV to far infrared (far-IR) region. In visible and near-IR region, KH_2PO_4 (KDP), KTiOPO_4 (KTP), and LiNbO_3 (LN) [4–6] are some excellent materials. $\beta\text{-BaB}_2\text{O}_4$ ($\beta\text{-BBO}$), LiB_3O_5 (LBO), and $\text{KBe}_2\text{BO}_3\text{F}_2$ (KBBF) as three “Chinese brand” crystals [7–9] are excellent NLO materials in UV and deep-UV region. Yet the application of the commercially available NLO crystals in the middle IR (mid-IR) region, such as AgGaS_2 and AgGaSe_2 , was limited mainly due to their comparatively much lower laser damage threshold (LDT). As a result, these crystals are damaged quickly upon irradiation of the lasers.

Although the mechanism for laser damage has not been completely clarified, two types of effects have been accepted for it. These two types are thermal effect and electronic effect; both are due to electron absorption. It has been gradually recognized that the intrinsic reason (narrow band gap) and extrinsic reason (defects of crystals) have caused the low LDT. Therefore, two approaches may be taken to improve the LDT of the mid-IR NLO crystals. One is to improve the crystal quality through improving the crystal growth method of the current materials, and the other is to explore new materials with wide band gaps. Due to the important applications of the mid-IR NLO crystals in optical communications, IR spectroscopy, and high-energy laser system, the research to find new NLO materials with high damage resistance to the incident laser beam together with relatively large NLO coefficient, wide transparent range in the mid-IR region, and good stability to the environment has become an urgent and challenging task in the field and thus has attracted great attention worldwide. Some good progress has been achieved in the last decade or so, for which the Chinese scientists have made a considerable contribution in both aspects: improving the crystal growth technique and exploring new strategy to search for new mid-IR NLO crystals [10–19]. This paper

summarizes the recent research progress in China for mid-IR NLO crystals with high LDT. The work will be described and discussed in three types of materials: chalcopyrites, oxides, and halides. The emphasis is put on the design strategy and quality control of the crystals.

2 Progress in ternary chalcopyrites

Chalcogenide NLO crystals normally show large SHG response (e.g., AgGaS₂: $d_{36} = 24$ pm/V, AgGaSe₂: $d_{36} = 40$ pm/V) and wide transparency (AgGaS₂: 0.48–11.4 μm , AgGaSe₂: 0.76–17 μm), but their narrow band gaps cause the low LDT (0.015 GW/cm² for AgGaS₂ and 0.012 GW/cm² for AgGaSe₂) [20].

AgGaS₂ and AgGaSe₂ crystallize in the chalcopyrite structure, which belong to $I\bar{4}2d$ space group. To this type of semiconductors, the higher crystal quality will be helpful to improve their LDT. With this aim, some groups have tried to improve the crystal growth equipments and methods to obtain high-quality crystals.

Zhu Shifu at Sichuan University made lots of effects on the crystal growth of these two materials. They used the modified Bridgman technique in two-zone vertical furnace. Crack-free AgGaS₂ crystal ingot with 12 mm in diameter and 20 mm in length and AgGaSe₂ crystal ingot with 22 mm in diameter and 88 mm in length have been grown using the polycrystalline materials. The transmission in the range of 2 to 10.6 μm is 49% for AgGaS₂ and 62.4% for AgGaSe₂. Recently, they used the quartz ampoule descending method to grow the AgGaS₂ crystal. The cracking phenomenon from the anomalous expansion phenomenon of AgGaS₂ crystal has been overcome, and the large-sized and integrally AgGaS₂ crystal was obtained [21].

ZnGeP₂ also belongs to the chalcopyrite system. It has drawn much attention due to its excellent properties in OPO and IR NLO device application [22–24]. Liu Yanting at Shandong University obtained the ZnGeP₂ crystal with the dimension of 7 and 25 mm in length by Bridgman method with the synthesized polycrystalline material [25]. Recently, the ZnGeP₂ crystals of larger size and higher quality were grown by Zhu Shifu at Sichuan University [26] and Tao Xutang at Shandong University, respectively [27].

In the past few years, some ternary chalcogenides containing lithium element, such as LiGaS₂ (LGS) and LiInS₂ (LIS) [28,29], have been discovered. The replacement of silver cation with main-group cationic elements, such as Li⁺ ion, increases their band gap and leads to a much higher LDT. LIS crystallizes in the spialterite structure belonging to $Pna2_1$ space group. It has a wide transparency in 0.35 to 13 μm

region, large NLO coefficient ($d_{33} = 15.8$ pm/V), and high LDT (> 0.1 GW/cm² at 1064 nm, 10 ns). As a unique IR NLO crystal, LIS possesses a nearly isotropic thermal expansion behavior and its thermal conductivity is about five times larger than that of AgGaS₂ [30]. It was first synthesized by G.D. Boyd in early 1973 [31], but it was very difficult to get good quality crystals. Some research groups in China have paid a lot of efforts on the crystal growth of LIS.

Tao Xutang at Shandong University has grown LIS crystals by the modified Bridgman method with accelerated crucible rotation technique (ACRT) using high-purity single-phase polycrystalline materials synthesized by autoclave method. After 2 weeks, high-quality and integrated LIS crystal with diameter of 12 mm and length of 40 mm was obtained [10].

The discovery of LIS and the theoretical study indicated that the replacement of main-group elements can effectively enlarge the band gap of the chalcogenide crystal. With the inspiration of this, some groups tried to increase the LDT by this strategy. Ye Ning at Fujian Institute of Research on the Structure of Matter selected BaGa₄S₇ as another potential IR NLO material for research. BaGa₄S₇ was first synthesized by Eisenmann et al. in 1983 and its single crystal structure belongs to $Pmn2_1$ space group (Fig. 1) [32]. Ye used the Bridgman-Stockbarger technique to grow BaGa₄S₇ from the polycrystalline materials that were synthesized from BaS, Ga, and S as the initial materials by solid-state reactions. Its UV and IR optical absorption edges were found to be at 350 nm and 13.7 μm , respectively. They calculated the NLO coefficient d_{33} to be about 12.6 pm/V from the powder SHG intensity. From the measurements, the band-gap energy of BaGa₄S₇ crystal is about 3.54 eV. In comparison to AgGaS₂ (2.64 eV) and ZnGeP₂ (1.75 eV), BaGa₄S₇ crystal has a relatively large band-gap energy, and the LDT of the BaGa₄S₇ single crystal reached about 1.2 J/cm² (0.12 GW/cm²) at 1.064 μm (Table 1) [11].

In addition to the discovery of new chalcogenides mid-IR NLO materials, quantum chemical calculations on the linear and nonlinear optical properties of known mid-IR NLO materials are also important for the rational design of the new materials. Lin Zheshuai and Chen Chuangtian at Beijing Technical Institute of Physics and Chemistry, CAS, have performed theoretical calculations on the band structures, birefractive indexes and nonlinear optical coefficients of chalcogenides, AgGaX₂ and LiGaX₂ (X = S, Se and Te) [33–35]. It was found that the reason for Li-containing crystals to exhibit the higher LDT value than that of Ag-containing crystals is that the d -orbitals of silver ion enter into the very top of the valence band of the Ag-containing crystals while no Li orbital lies at the band gap edge in the Li-containing crystals [34].

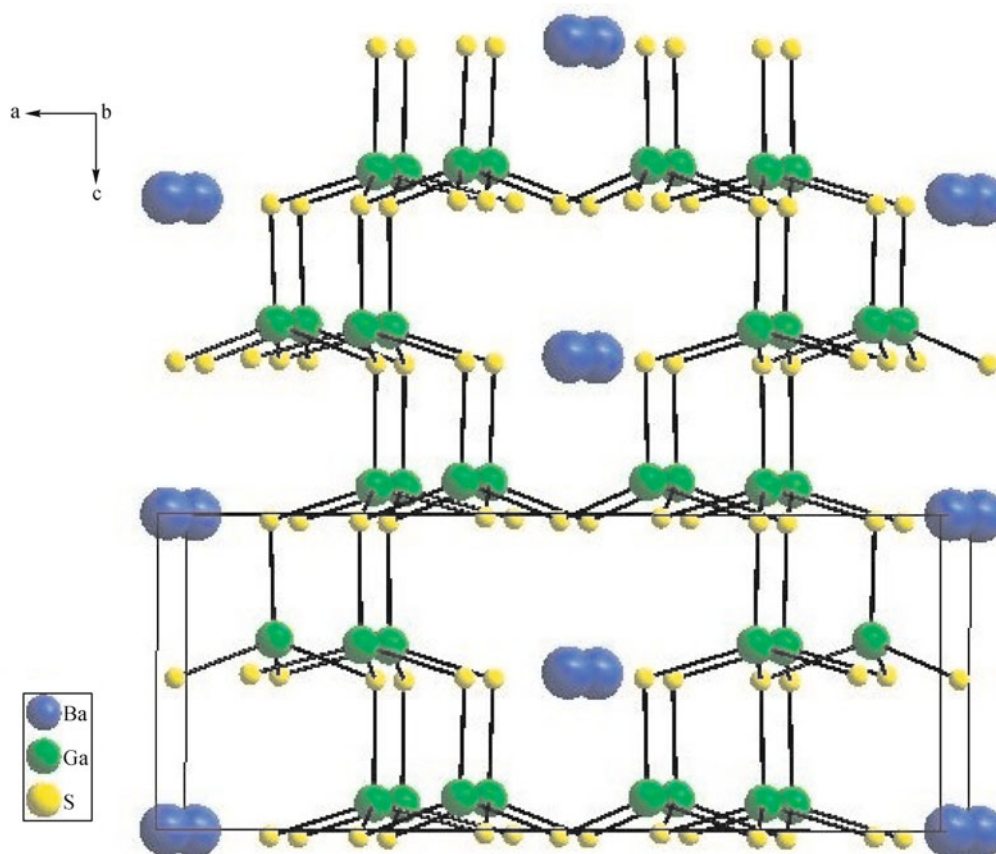


Figure 1 Crystal structure of BaGa₄S₇.

Table 1 Comparison of important parameters of selected crystals (See Ref. [11]).

crystal	point group	UV absorption edge/nm	IR absorption edge/ μm	NLO coefficient/ $\text{pm}\cdot\text{V}^{-1}$	LDT at 1.064 $\mu\text{m}/\text{J}\cdot\text{cm}^{-2}$
LiInS ₂	C_{2v}	410	12	16 (d_{33})	1
AgGaS ₂	D_{2d}	500	13.0	13 (d_{14})	0.4
ZnGeP ₂	D_{2d}	740	12.0	75.4 (d_{14})	0.03
BaGa ₄ S ₇	C_{2v}	350	13.7	12.6 (d_{33})	1.2

3 Progress in oxides

With the effective research on new chalcogenides, the LDT values have been improved but still not high enough for some applications. Compared to the semiconductive chalcogenides, many oxides are normally insulators, and the band gaps are normally much larger than that of chalcogenides. Meanwhile, oxides show some other advantages, such as diversity of structure, large distortions in crystal structure, good stability in air, and easy for crystal growth. However, oxides also have a disadvantage in the transparency in IR region since the atomic mass of oxygen is small. This can be improved by using heavy metal elements as the central cations. Therefore, oxides as potential mid-IR NLO materials have re-entered people's vision.

Chen Xue'an at Beijing University of Technology systematically studied new iodate NLO materials. LiMoO₃(IO₃) was synthesized under mild hydrothermal conditions. It shows SHG effect of about $4 \times$ KDP and its band edge is roughly 2.8 eV. Its transparent range is from 2.5 to 10.8 μm , and it is thermally stable up to at least 430°C [36].

Mao Jianggao at Fujian Institute of Research on the Structure of Matter synthesized many noncentrosymmetric oxides, and some of them showed good potential as mid-IR NLO materials. BaNbO(IO₃)₅ was synthesized by using hydrothermal reaction at 230°C for 4 days. It crystallizes in the acentric space group Cc (Fig. 2). This compound has a large SHG response about 14 times that of KDP and has a relatively wide band gap of 3.64 eV (AgGaS₂ = 2.64 eV and ZnGeP₂ = 1.75 eV) (Fig. 3). With the larger band gap, the

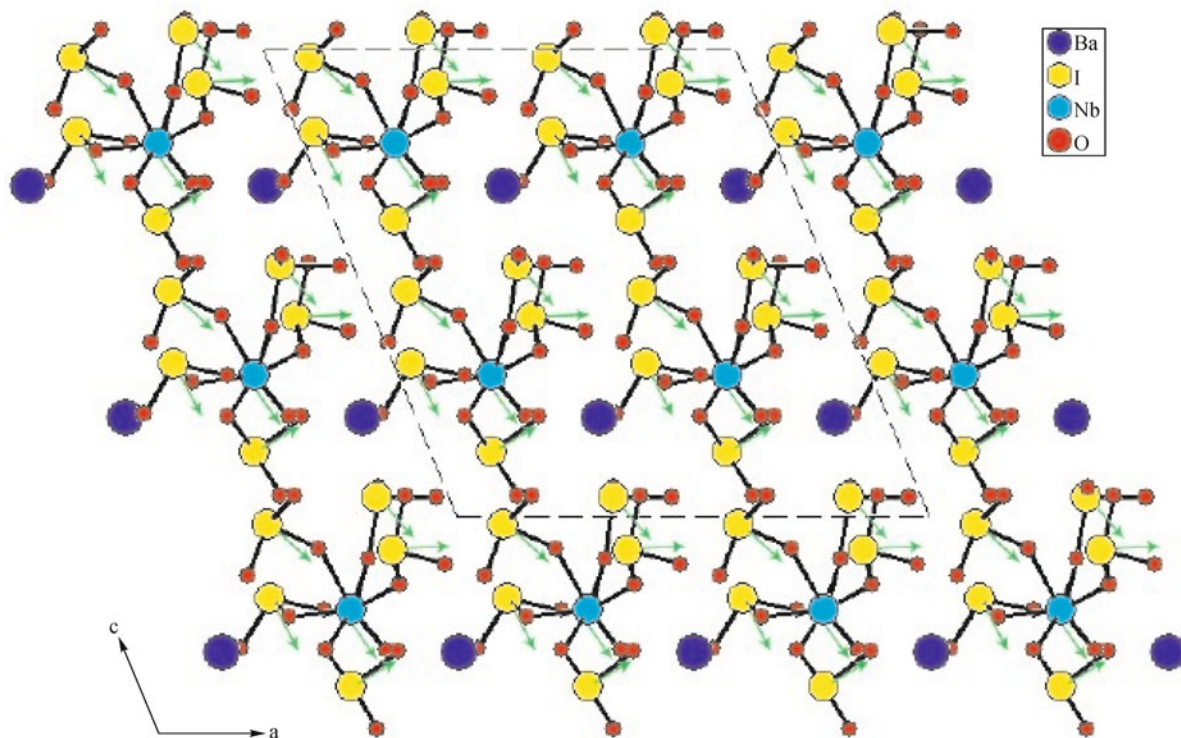


Figure 2 Crystal structure of $\text{BaNbO}(\text{IO}_3)_5$. Figure was reprinted with permission from Ref. [37].

LDT should be increased. Meanwhile, $\text{BaNbO}(\text{IO}_3)_5$ has a wide transparency wavelength range from 2.5 to 10 μm [37].

The above iodates are potential NLO materials for mid-IR. However, their single crystals of large size are difficult to obtain since the iodate compounds will be decomposed at high temperatures. Many iodate crystals can only be grown from solution, and the sizes of the crystals are always relatively small. How to find a suitable technique to grow large single crystal is another challenge for iodates to be used as mid-IR NLO materials.

BaTeM_2O_9 ($M = \text{Mo}$ or W) was first synthesized by Halasyamani at Houston University using the solid-state reaction [38]. The group has synthesized a lot of noncentrosymmetric oxides with d^0 transition-metal cations with lone pair of electrons under the guidance of second-order Jahn-Teller (SOJT) distortion effect. BaTeM_2O_9 showed SHG response as strong as about $15 \times \text{KH}_2\text{PO}_4$ (KDP). For the first time, Tao Xutang has successfully grown large-sized (30 mm \times 23 mm \times 18 mm) single crystal of $\text{BaTeMo}_2\text{O}_9$ from the TeO_2 - MoO_3 flux system (Fig. 4) [39]. The transmission spectra suggest that it transmits well from 0.5 to 5.0 μm . They found that thermal expansion of $\text{BaTeMo}_2\text{O}_9$ exhibits weak anisotropy although it belongs to low symmetry system, and the thermal conductivity of $\text{BaTeMo}_2\text{O}_9$ ascends as the temperature is increased as well [40]. These properties enable

$\text{BaTeMo}_2\text{O}_9$ to be another promising NLO material for the wavelength 3 to 5 μm in the IR region.

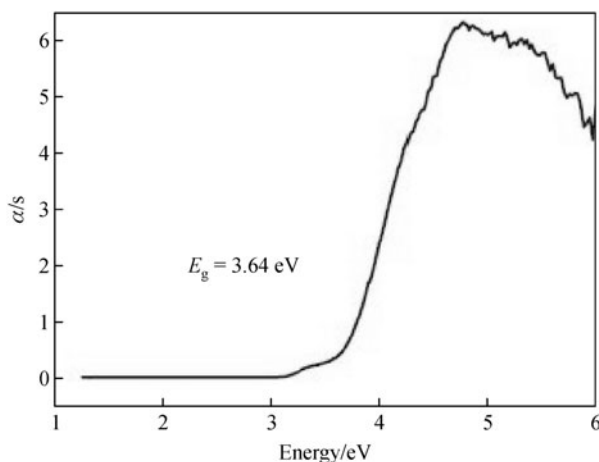


Figure 3 Band-gap feature of $\text{BaNbO}(\text{IO}_3)_5$. Figure was reprinted with permission from Ref. [37].

4 Progress in halides

Halides normally have large band gaps with versatile structures and relatively high stability. They are normally

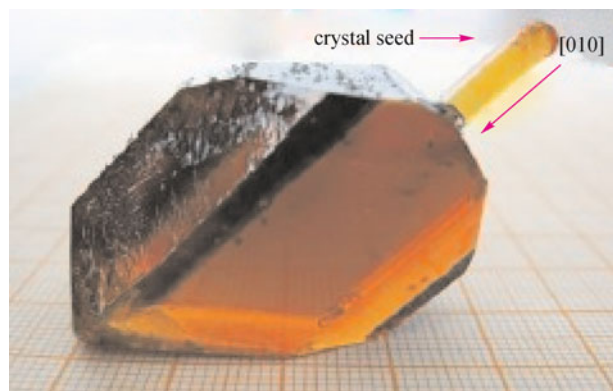


Figure 4 The as-grown bulk $\text{BaTeMo}_2\text{O}_9$ crystal. Figure was reprinted with permission from Ref. [39].

water-soluble and the big-sized single crystals may be grown in solution. Furthermore, the atomic mass of some halogens can be quite heavy, with which the halide compounds may exhibit wide transparent range in the mid-IR region. Therefore, halides may be another type of NLO materials with high LDT in mid-IR region.

Our group has been one of the pioneer groups in the study of halide mid-IR NLO crystals. The first halide we studied was CsGeCl_3 , the crystal structure of which was known before with a space group $R\bar{3}m$. Its NLO property was first and independently investigated by us [41] and Rosker [42]. In the

crystal, the anionic groups (GeCl_3^-) are arranged totally parallel, and Ge^{2+} ion has a lone pair of electron in its frontier orbital (Fig. 5). These facts are favorable to the second-order NLO property. It showed the powder SHG efficiency five times that of KDP with the wide transparency range within 0.4 to 20 μm . However, it is very difficult to grow large single crystals. Soon after we had published the above preliminary results, Fang et al. in Shandong University obtained 5 mm \times 5 mm \times 5 mm crystals of CsGeCl_3 from a HCl-EtOH-CsCl mixture solution and measured its LDT to be 200 MW/cm^2 [43].

Then Lin in National Chiao Tung University had paid attention to the mixed halides $\text{CsGeBr}_x\text{Cl}_{3-x}$ [44] and found that $\text{CsGeBr}_x\text{Cl}_{3-x}$ ($x = 0$) showed phase-matchable powder SHG of 14 times that of KDP.

Since the Ge^{2+} cation may not be stable toward oxidation to Ge^{4+} , we started to study the terhalides with Cd^{2+} or Hg^{2+} as central ions, which are more stable. CsCdBr_3 was a known compound reported as a centrosymmetric crystal structure in 1977 [45]. We used CsBr and CdI_2 as starting agents in water and wished to obtain CsCdBr_2 . However, the single crystal we got is CsCdBr_3 , which crystallizes with a non-centrosymmetric space group $P6_3mc$ [46]. It showed a powder SHG response three times that of KDP, with a transparent region in 0.3 to 20 μm . For Hg^{2+} as central cation, we focused on $\text{Cs}_2\text{Hg}_3\text{I}_8$ and HgBr_2 . Single crystal $\text{Cs}_2\text{Hg}_3\text{I}_8$

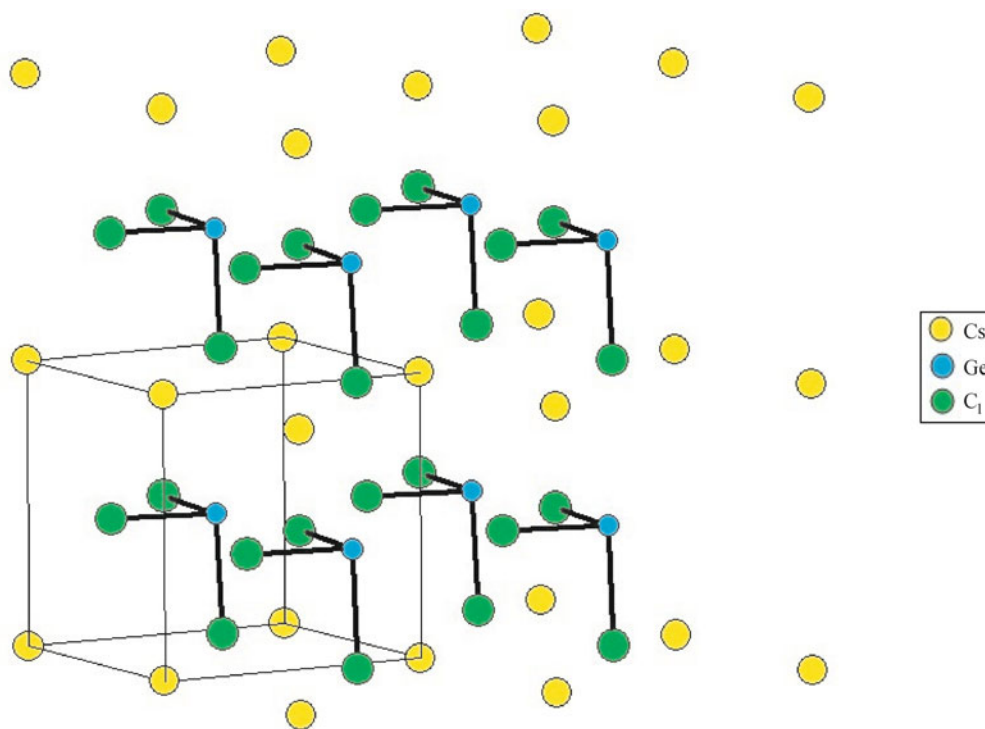


Figure 5 Crystal structure of CsGeCl_3 .

with the size $25 \text{ mm} \times 14 \text{ mm} \times 5 \text{ mm}$ has been grown in acetone by a slow evaporation technique. It showed a powder SHG as strong as KTP with a transparent region within $0.5\text{--}25 \mu\text{m}$ [21]. For HgBr_2 , both Hg and Br are heavy elements and the difference of electro-negativity between these two elements may be favorable to the good stability and high LDT. The results indicated that HgBr_2 showed a phase-matchable powder SHG intensity as strong as 11 times that of KDP, and it is transparent in the region of $0.4\text{--}20 \mu\text{m}$. The crystal has been grown from EtOH solution and the LDT was determined to be 300 MW/cm^2 [17].

Among the halides, the fluorides show widest band gap owing to the strongest electro-negativity of fluorine. To further enhance the LDT, fluorine atom can be used to replace the other halogen atom. On the other hand, however, fluorides normally show the weakest NLO effect, since fluorine atom has a strong ability to constrain the outer electrons. We first chose Sb^{3+} as a cation since it contains a lone electron pair, which is favorable for NLO, and studied the possibility of SbF_3 for NLO application. This compound showed phase-matchable SHG 5.8 times that of KDP with the transparency within $0.29\text{--}12 \mu\text{m}$ range [19]. The band gap of SbF_3 was about 4.3 eV , which is quite large. Relatively large-sized

single crystals can be grown from aqueous hydrogen fluoride solution, but it is hygroscopic.

To avoid the hygroscopic behavior shown in SbF_3 , a sodium salt of antimony fluoride anion, $\text{NaSb}_3\text{F}_{10}$, was investigated. It was synthesized via the reaction of NaF with Sb_2O_3 in concentrated hydrogen fluoride solution and crystallized in the space group $P6_3$ (Fig. 6). It showed phase-matchable powder SHG 3.2 times that of KDP with a decomposition temperature over 200°C . The transparent region is 0.25 to $7.8 \mu\text{m}$, and the band gap is about 5.0 eV (Fig. 7). Single crystal of the size $12 \text{ mm} \times 10 \text{ mm} \times 8 \text{ mm}$ has been grown in aqueous solution by means of a slow evaporation technique (Fig. 8). The LDT value was determined to be 1.3 GW/cm^2 by a laser radiation at a wavelength $1.064 \mu\text{m}$ and the pulse of 8 ns [16]. This value is one order of magnitude higher than that of LiInS_2 ($\text{LiInS}_2 = 0.1 \text{ GW/cm}^2$).

5 Conclusions and perspective

For the past decades, Chinese research groups have made a valuable contribution toward the UV and visible NLO

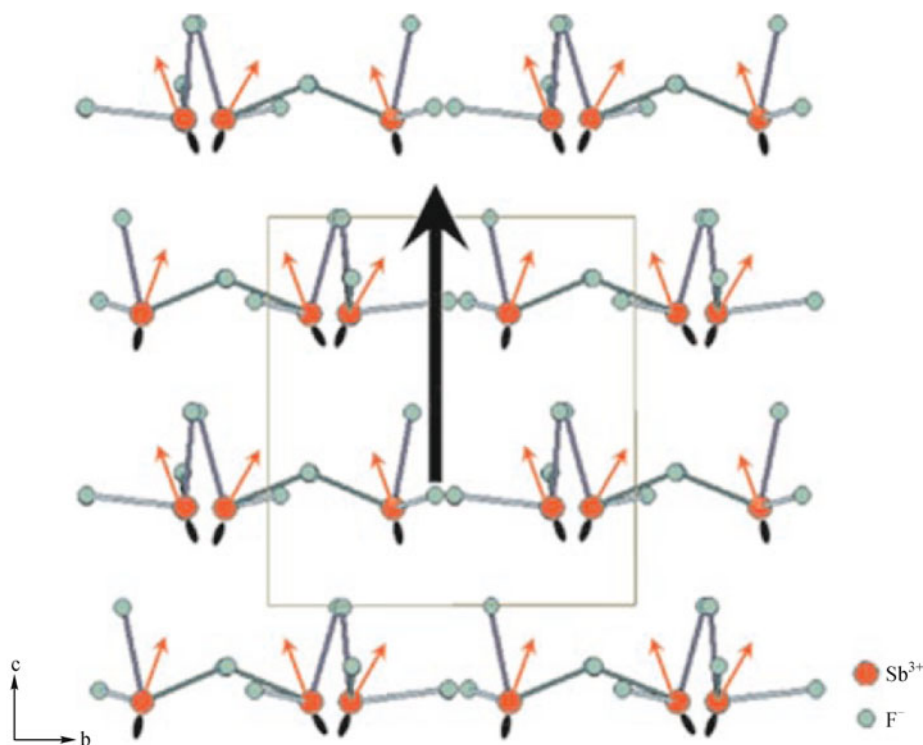


Figure 6 Crystal structure of $\text{Na}_3\text{Sb}_3\text{F}_{10}$. Figure was reprinted with permission from Ref. [16].

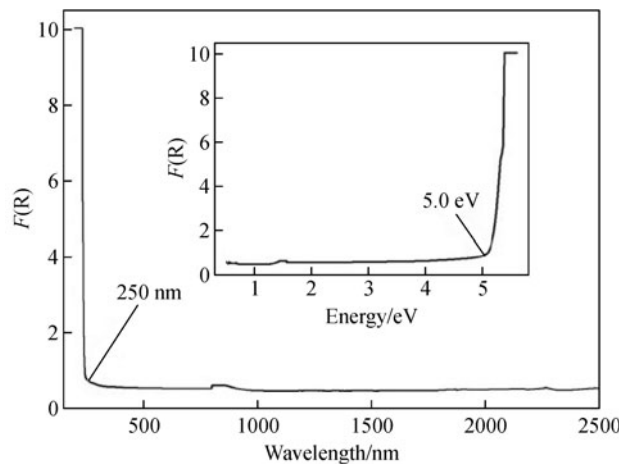


Figure 7 Band-gap feature of $\text{Na}_3\text{SbF}_{10}$. Figure was reprinted with permission from Ref. [16].

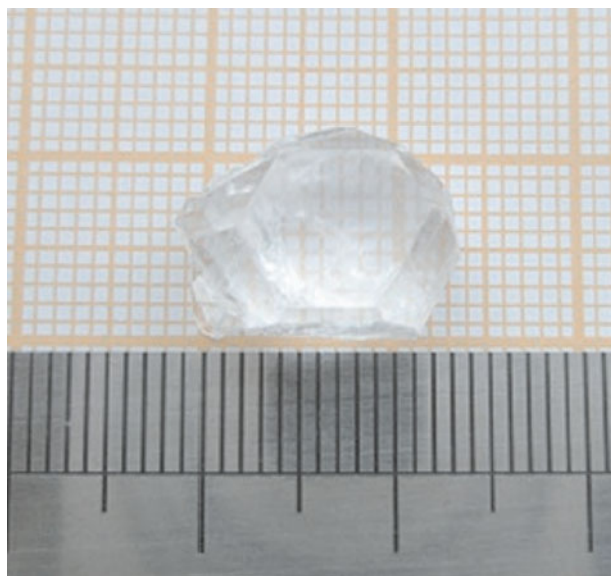


Figure 8 Photograph of grown $\text{Na}_3\text{SbF}_{10}$ crystal. Figure was reprinted with permission from Ref. [16].

crystals. Right now, they also commit themselves to the mid-IR NLO crystals and have made lots of effects. Chinese scientific researchers have excellent experiences on crystal growth and improved the crystal growth technologies of some known IR NLO crystals to enhance the crystal quality with the aim of achieving higher LDT. On the other hand, Chinese scientists also have strong ability to design new NLO crystals and explored the new mid-IR NLO crystals in three types of the compounds: chalcogenides, oxides, and halides. The progress has been encouraging and some new materials have shown great potential for future applications. However, there are still lots of work to be done for the practical applications

in mid-IR NLO field. The new materials must show simultaneously excellent comprehensive properties, such as large NLO efficiency, wide transparency region, large LDT, high stability, and easy to grow relatively large-sized crystals with high quality. This interdisciplinary area needs a joint effort from chemists, physicists, and material scientists. We believe that their collaboration in molecular engineering and crystal engineering will produce excellent new mid-IR NLO crystals in the near future.

Acknowledgements We gratefully acknowledge the efforts of the formal and current graduate students in our group and our collaborators, whose names are given in the references of this paper. This work was supported by the National Basic Research Project of China (No. 2010CB630701) and the National Natural Science Foundation of China (No. 91022036).

References

1. Franken, P. A.; Hill, A. E.; Peters, C. W.; Weinreich, G., *Phys. Rev. Lett.* **1961**, *7*, 118–119
2. Cyranoski, D., *Nature* **2009**, *457*, 953–955
3. Chen, C.; Lin, Z.; Wang, Z., *Appl. Phys. B* **2005**, *80*, 1–25
4. Smith, W. L.; Hickey, J.; Howell, H. B.; Jacobowitz, H.; Hilleary, D. T.; Drummond, A. J., *Appl. Opt.* **1977**, *16*, 306–318
5. Kato, K., *IEEE J. Quantum Electron.* **1991**, *27*, 1137–1140
6. Boyd, G. D.; Miller, R. C.; Nassau, K.; Bond, W. L.; Savage, A., *Appl. Phys. Lett.* **1964**, *5*, 234
7. Chen, C. T.; Wu, B. C.; Jiang, A.; You, G., *Sci. Sin. [B]* **1985**, *28*, 235
8. Chen, C. T.; Wu, Y. C.; Jiang, A.; Wu, B. C.; You, G.; Li, R. K.; Lin, S. J., *J. Opt. Soc. Am. B* **1989**, *6*, 616
9. Chen, C.; Xu, Z.; Deng, D.; Zhang, J.; Wong, G. K. L.; Wu, B.; Ye, N.; Tang, D., *Appl. Phys. Lett.* **1996**, *68*, 2930
10. Wang, S.; Tao, X.; Dong, C.; Jiao, Z.; Jiang, M. *Chinese J. Struct. Chem.* **2007**, *26*, 1184
11. Lin, X.; Zhang, G.; Ye, N., *Cryst. Growth Des.* **2009**, *9*, 1186–1189
12. Phanon, D.; Gautier-Luneau, I., *Angew. Chem. Int. Ed.* **2007**, *46*, 8488–8491
13. Wang, S.; Tao, X.; Dong, C.; Jiao, Z.; Jiang, M., *J. of Synthetic Cryst* **2007**, *36*, 8
14. Zhao, B.; Zhu, S.; Li, Z.; Fu, S.; Yu, F.; Li, Q., *J. of Synthetic Cryst* **1999**, *28*, 4
15. Wang, M.; Yang, C.; Lei, Z.; Xia, S.; Zhu, C.; Sun, L.; Zhou, Y., *Cryst. Res. Technol.* **2010**, *45*, 25–30
16. Zhang, G.; Qin, J.; Liu, T.; Li, Y.; Wu, Y.; Chen, C., *Appl. Phys. Lett.* **2009**, *95*, 261104/1
17. Liu, T.; Qin, J.; Zhang, G.; Zhu, T.; Niu, F.; Wu, Y.; Chen, C., *Appl. Phys. Lett.* **2008**, *93*, 091102/1
18. Zhang, G.; Liu, T.; Qin, J.; Fu, P.; Wu, Y.; Chen, C., *Cryst. Growth Des.* **2008**, *8*, 2946–2949
19. Zhang, G.; Liu, T.; Zhu, T.; Qin, J.; Wu, Y.; Chen, C., *Opt.*

- Mater.* **2008**, *31*, 110–113
20. Dmitriev, V. G.; Gurzadyan, G. G.; Nikogosyan, D. N., *Handbook of Nonlinear Optical Crystals*, 2nd Ed.; Springer-Verlag: Berlin, **1995**
21. Yuan, Z.; Zhu, S.; Zhao, B.; Chen, B.; He, Z.; Yang, S., *J of Synthetic Cryst* **2009**, *38*, 1
22. Jiang, Y.; Ding, Y. J., *Opt. Express* **2007**, *15*, 12699–12707
23. Henriksson, M.; Tiuhonen, M.; Pasiskevicius, V.; Laurell, F., *Appl. Phys. B* **2007**, *88*, 37–41
24. Zawilski, K. T.; Schunemann, P. G.; Setzler, S. D.; Pollak, T. M., *J. Cryst. Growth* **2008**, *310*, 1891–1896
25. Lin, Y.; Gu, Q.; Liu, H.; Zhang, H.; Ge, W.; Fang, C.; Hu, X.; Wang, J., *Function Mater* **2006**, *37*, 864
26. Zhao, X.; Zhu, S. F.; Zhao, B. J.; Chen, B. J.; He, Z. Y.; Wang, R. L.; Yang, H. G.; Sun, Y. Q.; Cheng, J., *J. Cryst. Growth* **2008**, *311*, 190–193
27. Zhang, G. D.; Tao, X. T.; Wang, S. P.; Liu, G. D.; Shi, Q.; Jiang, M. H., In: Proceedings of the 16th international conference on crystal growth/14th international conference on vapor growth and epitaxy (ICCG-16/ICVGE-14), August 8th, 2010, Beijing, PB131
28. Isaenko, L.; Yelisseyev, A.; Lobanov, S.; Krinitsin, P.; Petrov, V.; Zondy, J. J., *J. Non-Cryst. Solids* **2006**, *352*, 2439–2443
29. Isaenko, L.; Vasilyeva, I.; Merkulov, A.; Yelisseyev, A.; Lobanov, S., *J. Cryst. Growth* **2005**, *275*, 217–223
30. Isaenka, L.; Yelisseyev, A.; Lobanova, S.; Petrovc, V.; Rotermunde, V. F.; Zondyd, J. J.; Knippelse, G. H., M., *Mater. Sci. Semicond. Process.* **2001**, *4*, 664
31. Boyd, G. D.; Kasper, H. M.; McFee, J. H., *J. Appl. Phys.* **1973**, *44*, 2809
32. Eisenmann, B.; Jakowski, M.; Schaefer, H., *Rev. Chim. Miner* **1983**, *20*, 329
33. Bai, L.; Lin, Z. S.; Wang, Z. Z.; Chen, C. T.; Lee, M. -H., *J. Chem. Phys.* **2004**, *120*, 8772–8778
34. Bai, L.; Lin, Z. S.; Wang, Z. Z.; Chen, C. T., *J. Appl. Phys.* **2008**, *103*, 083111
35. Atuchin, V. V.; Lin, Z. S.; Isaenko, L. I.; GKesler, V.; NKruchinin, V.; Lobanov, S. I., *J. Phys. Condens. Matter* **2009**, *21*, 455502
36. Chen, X. A.; Zhang, L.; Chang, X. A.; Xue, H. P.; Zang, H. G.; Xiao, W. Q.; Song, X. M.; Yan, H., *J. Alloy. Comp.* **2007**, *428*, 54–58
37. Sun, C. F.; Hu, C. L.; Xu, X.; Ling, J. B.; Hu, T.; Kong, F.; Long, X. F.; Mao, J. G., *J. Am. Chem. Soc.* **2009**, *131*, 9486–9487
38. Ra, H. S.; Ok, K. M.; Halasyamani, P. S., *J. Am. Chem. Soc.* **2003**, *125*, 7764–7765
39. Zhang, W. G.; Tao, X. T.; Zhang, C. Q.; Gao, Z. L.; Zhang, Y. Z.; Yu, W. T.; Cheng, X. F.; Liu, X. S.; Jiang, M. H., *Cryst. Growth Des.* **2008**, *8*, 304–307
40. Zhang, W. G.; Tao, X. T.; Zhang, C. Q.; Zhang, H. J.; Jiang, M. H., *Cryst. Growth Des.* **2009**, *9*, 2633–2636
41. Zhang, J.; Qin, J., *SPIE* **1998**, *3556*, 1
42. Rosker, M. J.; Cunningham, P. H.; Ewbank, M. D.; Gunter, P., *U. S.* **1998**, 6 pp
43. Gu, Q.; Pan, Q.; Wu, X.; Shi, W.; Fang, C., *J. Cryst. Growth* **2000**, *212*, 605–607
44. Lin, Z. G.; Tang, L. C.; Chou, C. P., *Inorg. Chem.* **2008**, *47*, 2362–2367
45. Moller, C. K.; Saarinen, H.; Näsäkkälä, E.; Pouchard, M.; Hagenmuller, P.; Andresen, A. F., *Acta Chem. Scand. A* **1977**, *31*, 669–672
46. Ren, P.; Qin, J.; Chen, C., *Inorg. Chem.* **2003**, *42*, 8–10